Available online at www.sciencedirect.com
ScienceDirect
Bioorganic & Medicinal Chemistry 16 (2008) 1006–1014
Bioorganic & Medicinal Chemistry

Synthesis, DNA binding, and cytotoxicity of 1,4-bis(2-amino-ethylamino)anthraquinone–amino acid conjugates

Ling-Wei Hsin,[a,*] Hui-Po Wang,[b,†] Pi-Hung Kao,[a] On Lee,[a] Wan-Ru Chen,[a] Hung-Wei Chen,[a] Jih-Hwa Guh,[a] Ya-Ling Chan,[a] Chin-Ping His,[a] Ming-Show Yang,[b] Tsai-Kun Li[c] and Chieh-Hua Lee[c]

[a]*Institute of Pharmaceutical Sciences, College of Medicine, National Taiwan University, No. 1, Section 1, Jen-Ai Road, Room 1336, Taipei 10018, Taiwan, ROC*
[b]*Institute of Natural Product, Chang Gung University, 259 Wen-Hwa 1st Road, Taoyuan 333, Taiwan, ROC*
[c]*Department and Graduate Institute of Microbiology, College of Medicine, National Taiwan University, No. 1, Section 1, Jen-Ai Road, Taipei 10018, Taiwan, ROC*

Received 8 July 2007; revised 1 October 2007; accepted 4 October 2007
Available online 10 October 2007

Abstract—Two series of 1,4-bis(2-amino-ethylamino)anthraquinone–amino acid conjugates (BACs), ametantrone (AT)–amino acid conjugates (AACs) and mitoxantrone (MX)–amino acid conjugates (MACs), were designed and synthesized. The DNA binding of BACs was evaluated by DNA thermal denaturation experiment. In the series, the methionine-substituted BACs had the weakest DNA binding, while the lysine-substituted BACs had the highest T_m values. The abilities of BACs to inhibit the growth of MCF-7, NCI-H460, SF-268, and PC-3 cell lines were determined. L-Met–MAC **16** and L-Lys–MAC **20** were the most potent growth inhibitors. MAC **16** was more cytotoxic than MX, whereas the T_m of MAC **16** was much lower than that of MX. In contrast to MAC **16**, L-Lys–MAC **20** demonstrated higher T_m than MX. These data suggested that Met–BACs possessed a different pharmacological profile, in which the ability to stabilize DNA is not parallel to the ability to kill cancer cells, from that of AT and MX. The primary mechanism of cytotoxicity for MAC **16** was most likely through TOP2 poisoning. Therefore, MAC **16** may provide a lead for the development of novel generations of anthraquinone-type antitumor agents.

1. Introduction

1,4-Disubstituted anthraquinones, such as ametantrone (AT) and mitoxantrone (MX), demonstrate potent antitumor activity and have been used widely in clinic since 1980s.[1,2] In addition, MX has been the only drug approved by the FDA for the treatment of worsening relapsing-remitting multiple sclerosis (MS), secondary progressive MS, and progressive-relapsing MS since 2000.[3,4] However, these clinical applications are limited due to the accumulative and irreversible cardiotoxicity.[2–4] Recently, MX was found to induce a progressive increase in mitochondrial mass in the cancer cells but not in the cardiac cells.[5] This suggests the opportunities to develop novel anthraquinones with reduced cardiotoxicity.

The planar tricyclic structure of anthraquinone is essential for intercalating into DNA base pairs. The two side chains of AT and MX could be used to connect with a variety of substituents, which may form additional interactions with the double-stranded DNA (ds-DNA) or DNA-topoisomerase II (TOP2) cleavable complex to increase their binding affinities and selectivities. It is well known that precise recognition of defined DNA sequences in biological systems is mediated by enzymes and proteins having appropriate structure motifs.[6] In the literature, various anthraquinone–peptide conjugates[7–11] and bis-amino acid-substituted anthraquinone conjugates[12,13] were reported to demonstrate remarkable DNA binding and exhibit cytostatic or cytotoxic activities. In addition, mono-amino acid-substituted anthraquinone conjugates could inhibit the catalytic activity of TOP1 and TOP2.[14,15] Theoretical design of anthraquinone–oligopeptide conjugates to selectively

Keywords: Anthraquinone; DNA binding; DNA affinity; Conjugate; Cytotoxicity.
* Corresponding author. Tel.: +886 2 2395 2310; fax: +886 2 2351 2086; e-mail: lwhsin@ntu.edu.tw
† Current address: College of Pharmacy, Taipei Medical University, 250 Wu-Hsing St., Taipei 110, Taiwan, ROC.

0968-0896/$ - see front matter © 2007 Elsevier Ltd. All rights reserved.
doi:10.1016/j.bmc.2007.10.012

target the double-stranded oligonucleotides has also been published.[16,17]

With the aim to discover more specific chemotherapeutic agents, a focused library of 1,4-bis(2-amino-ethylamino)anthraquinone–amino acid conjugates (BACs) was designed and synthesized. The α-amino acids possessing a variety of side chains, which could be used to create specific interactions by one of the following mechanisms, were chosen for construction of BACs.

(1) Metal ions, such as magnesium and zinc, are involved in DNA synthesis and repair processes. Attaching the amino acids containing potential metal ion-chelating side chain (i.e., the methylsulfanyl group of methionine) to the core structure may be useful to interrupt DNA synthesis by stabilization of the DNA–TOP2 cleavable complex.
(2) The hydroxyl group of tyrosine residue in TOP2 plays an essential role in TOP2-mediated DNA strand cleavage.[18,19] Furthermore, the side chains of AT and MX also contain the hydroxyl groups. Therefore, introducing hydroxyl group-containing amino acids (i.e., serine and tyrosine) to anthraquinone may provide the opportunity to enhance the cytotoxicity of this series of BACs.
(3) The ε-amino group of lysine is protonated under physiological conditions, which would be expected to produce strong electrostatic interactions with the negatively charged phosphate groups on DNA skeleton.[12,13]

In this paper, we report the synthesis, DNA binding, and in vitro cytotoxicity of two series of L- or D-amino acid-conjugated BACs, AT–amino acid conjugates (AACs) and MX–amino acid conjugates (MACs) (Chart 1).

2. Chemistry

AACs **1**–**14** and MACs **15**–**20** (Chart 2) were synthesized starting from leucoquinizarin (**21**) and 5,8-dihydroxy-leucoquinizarin (**22**), respectively. As compound **22** was not commercially available, 1,5-diamino-4,8-dihydroxyanthraquinone was used to prepare **22** according to the literature procedure.[20] Treatment of **21** and **22** with an excess amount of mono-*N*-*t*-Boc-protected ethylenediamine in methanol, followed by air oxidation, afforded bis-*N*-*t*-Boc-protected **23** and **24**, respectively, as shown in Scheme 1.[8,21–23] Trifluoroacetic acid (TFA)-catalyzed deprotection of **23** and **24** provided key intermediates 1,4-bis(2-amino-ethylamino)anthra-

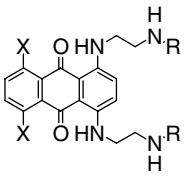

1: X = H; R = *N*-α-*tert*-Boc-L-methioninyl
2: X = H; R = L-methioninyl (2TFA)
3: X = H; R = *N*-α-*tert*-Boc-D-methioninyl
4: X = H; R = D-methioninyl (2TFA)
5: X = H; R = *N*-α-Fmoc-*O*-*tert*-butyl-L-serinyl
6: X = H; R = *O*-*tert*-butyl-L-serinyl
7: X = H; R = L-serinyl (2TFA)
8: X = H; R = *O*-*tert*-butyl-L-tyrosinyl
9: X = H; R = L-tyrosinyl (2TFA)
10: X = H; R = *N*-α,ε-di-*tert*-Boc-L-lysinyl
11: X = H; R = L-lysinyl (4TFA)
12: X = H; R = *N*-α-Fmoc-*N*-ε-*tert*-Boc-D-lysinyl
13: X = H; R = *N*-ε-*tert*-Boc-D-lysinyl
14: X = H; R = D-lysinyl (4TFA)

15: X = OH; R = *N*-α-*tert*-Boc-L-methioninyl
16: X = OH; R = L-methioninyl (2TFA)
17: X = OH; R = *N*-α-*tert*-Boc-D-methioninyl
18: X = OH; R = D-methioninyl (2TFA)
19: X = OH; R = *N*-α,ε-di-*tert*-Boc-L-lysinyl
20: X = OH; R = L-lysinyl (4TFA)

Chart 2.

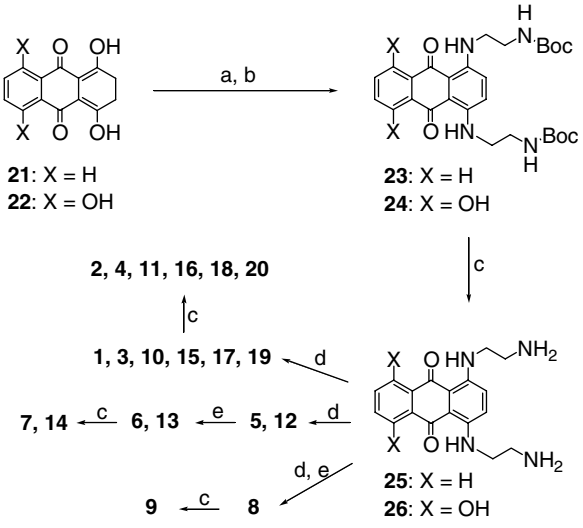

Scheme 1. Reagents and conditions: (a) $BocNHCH_2CH_2NH_2$, CH_3OH, 50 °C; (b) air, CH_3OH, 45 °C; (c) TFA, CH_2Cl_2, rt; (d) corresponding protected amino acids, DCC, HOBt, CH_2Cl_2, rt; (e) piperidine, CH_2Cl_2, rt.

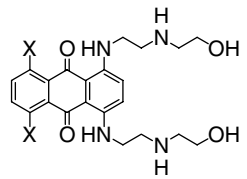

Ametantrone (**AT**): X = H
Mitoxantrone (**MX**): X = OH

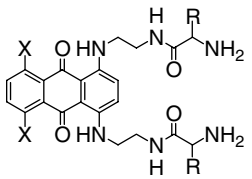

Ametantrone-Amino acid Conjugate (**AAC**): X = H
Mitoxantrone-Amino acid Conjugate (**MAC**): X = OH

Chart 1.

quinone (**25**) and 1,4-bis(2-amino-ethylamino)-5,8-dihydroxy-anthraquinone (**26**) in quantitative yields.

Both of the AACs and MACs were prepared via a general reaction sequence (Scheme 1). Coupling of compounds **25** and **26** with appropriate *N*- and side chain-protected amino acids using *N*,*N*′-dicyclohexylcarbodiimide (DCC) in the presence of *N*-hydroxybenzotriazole (HOBt), *N*-hydroxyphthalimide, or *N*-hydroxysuccinimide produced protected BACs in moderate yields. In consideration of both the shorter reaction time and easier purification process, HOBt provided the most satisfactory results. The *N*-*t*-Boc and *O*-*t*-Bu protective groups of BACs were removed using 20–50% TFA in CH_2Cl_2, while the *N*-9-fluorenylmethoxycarbonyl (Fmoc) protective group was cleaved by 10% piperidine in CH_2Cl_2.

3. Pharmacology

Effective intercalating agents, such as anthraquinone derivatives, are well known for their ability to raise the melting temperature (T_m) of ds-DNA.[24,25] Although the increases in T_m may not be directly correlated with DNA binding affinity,[26] higher ΔT_m values indicate tighter interactions between the ligand and ds-DNA.[24] Therefore, the DNA binding of BACs was evaluated by determination of their ability to alter the thermal denaturation profile of calf thymus DNA (ct-DNA).[8,24–28] In general, the BACs with C log *P* values larger than 3.5 were not soluble enough in BPE buffer. Therefore, the T_m for those highly lipophilic BACs could not be determined. The ΔT_m values of the BACs with sufficient solubility were measured and the results of melting experiments are shown in Table 1.

L-Lys- and D-Lys-substituted AACs **11** and **14** had larger ΔT_m values than AT, which is a potent DNA intercalator. When the distal amino groups (N^{ε}) were protected (i.e., **13**), the ΔT_m was significantly reduced. Therefore, the positively charged side chains of AACs **11** and **14** were important and the multiple ionic interactions with the negatively charged phosphate backbone of ds-DNA might be involved. In contrast to Lys-substituted AACs, the Met-substituted AACs**2** and **4** showed very weak DNA binding. Interestingly, the L-Met–AAC **2** and D-Met–AAC **4** possessed similar DNA stabilization ability, which means there was no significant chirality discrimination.

The ΔT_m values for the hydroxyl-containing L-Ser–AAC **7** and L-Tyr–AAC **9** were moderate and almost the same. Initially, we thought the additional hydrogen bonding to the DNA produced by the hydroxyl-containing side chains was responsible for the T_m change. However, the hydroxyl-protected L-Ser(*t*-Bu)–AAC **6** demonstrated a higher T_m than that of unprotected L-Ser–AAC **7** (6.5 and 5.4 °C, respectively) and therefore, the side chain hydroxyl groups might not be important for DNA binding in AAC series. The magnitude of ΔT_m values in the AAC series was in the following order: L-Lys, D-Lys >AT ≫ Ser(*t*-Bu) > Ser > Tyr > D-Lys(Boc) > D-Met > L-Met.

In previous structure–activity relationship (SAR) studies, 5,8-dihydroxy-anthraquinones were more potent than the non-hydroxylated analogs in antitumor activity.[20–22] In this study, the 5,8-dihydroxy-substituted MACs also had larger ΔT_m values than the corresponding AACs. It is noteworthy that when the solution of L-Lys–MAC **20** in normal concentration was added to the ct-DNA solution, deep blue aggregates were formed instantly which prohibited the determination of T_m. Therefore, the final concentration of **20** in the DNA–drug solutions for thermal denaturation study was reduced to 5 μM to estimate the DNA binding affinity of **20**. Even under this diluted condition, L-Lys–MAC **20** showed a very high ΔT_m value of 27.7 °C. MX displayed a similar but less aggregation phenomenon than MAC **20**. At a concentration of 10 μM, MX raised the melting temperature of ct-DNA by 25.3 °C. The L-Met- and D-Met-substituted MACs **16** and **18** also had higher T_m than the corresponding AACs **2** and **4**, although the ΔT_m values for Met-substituted MACs **16** and **18** were much less than that of L-Lys–MAC **20**.

Based on these results, the amino acid residues in BACs did play crucial role in the modulation of drug binding to ct-DNA. Smaller T_m shifts were observed for the non-ionic side chain-containing BACs. The larger ΔT_m values of Ser– and Tyr–AACs than of Met–AACs suggest that the terminal hydroxyl groups are likely to be favored for binding just as in the cases of AT and MX. In both the AAC and MAC series, the D- and L-BACs showed no significant differences in their DNA binding properties, which point to a poor chiral discrimination in the BAC–DNA complexes.

The results of in vitro cytotoxicity screening[29] of BACs **1**–**20** against MCF-7 (breast cancer), NCI-H460 (non-small cell lung carcinoma), SF-268 (glioblastoma), and PC-3 (prostate cancer) cell lines are reported in Table 2. In the AAC series, L-Met–AAC **2** had the most potent activity against PC-3 cell line (GI_{50} = 1.50 μM), while the corresponding *N*-protected L-Met–AAC **1** was inactive in this assay. *N*-Fmoc-*O*-*t*-Bu-protected L-Ser–AAC **5** was the most potent growth inhibitor for NCI-H460 in the AACs, while inactive for the other three cancer cell lines. Selective N-deprotection of AAC **5** provided *O*-*t*-Bu-protected L-Ser–AAC **6**, which showed moderate cytotoxicity against all cancer cell lines. Removing both protective groups of AAC **5** produced L-Ser–AAC **7**, which possessed the lowest C log *P* value (−1.74) among the BACs and was totally inactive in this assay. *O*-*t*-Bu-protected L-Tyr–AAC **8** and unprotected L-Tyr–AAC **9** were 2- to 3-fold more potent than AT in growth inhibition against PC-3 cell line, while did not show significant activity against MCF-7, NCI-H460, and SF-268 cell lines.

L-Lys–AAC **11** did not show significant cytotoxicity against the four cancer cell lines, although AAC **11** was an extraordinarily strong DNA binder. Interestingly, the N^{α}, N^{ε}-protected L-Lys–AAC **10** showed substantial growth inhibition activity against MCF-7, SF-268, and PC-3 cell lines. In PC-3 cell line, AAC **10** was four times more potent than AT (GI_{50} = 1.83, 8.52 μM, respectively). The lipophilicity and α-amino

Table 1. Clog *P* and ΔT_m values for BACs

No.	*N*-α PG	Amino acid	Side chain PG	Clog *P*[a]	ΔT_m (°C)[b,c]	Molecular formula
1	Boc	Met	—	4.22	ND	$C_{38}H_{54}N_6O_8S_2$
2	—	Met	—	0.57	1.4 ± 0.3	$C_{28}H_{38}N_6O_4S_2{\cdot}2C_2HF_3O_2$
3	Boc	D-Met	—	4.22	ND	$C_{38}H_{54}N_6O_8S_2$
4	—	D-Met	—	0.57	1.6 ± 0.3	$C_{28}H_{38}N_6O_4S_2{\cdot}2C_2HF_3O_2$
5	Fmoc	Ser	*t*-Bu	>6.00	ND	$C_{62}H_{66}N_6O_{10}$
6	—	Ser	*t*-Bu	1.98	6.5 ± 0.5	$C_{32}H_{46}N_6O_6$
7	—	Ser	—	−1.74	5.4 ± 0.1	$C_{24}H_{30}N_6O_6{\cdot}2C_2HF_3O_2$
8	—	Tyr	*t*-Bu	5.42	ND	$C_{44}H_{54}N_6O_6$
9	—	Tyr	—	1.77	5.2 ± 0.7	$C_{36}H_{38}N_6O_6{\cdot}2C_2HF_3O_2$
10	Boc	Lys	Boc	>6.00	ND	$C_{50}H_{76}N_8O_{12}$
11	—	Lys	—	−0.33	>25	$C_{30}H_{44}N_8O_4{\cdot}4C_2HF_3O_2$
12	Fmoc	D-Lys	Boc	>6.00	ND	$C_{70}H_{80}N_8O_{12}$
13	—	D-Lys	Boc	3.32	3.1 ± 0.1	$C_{40}H_{60}N_8O_8$
14	—	D-Lys	—	−0.33	>25	$C_{30}H_{44}N_8O_4{\cdot}4C_2HF_3O_2$
15	Boc	Met	—	3.86	ND	$C_{38}H_{54}N_6O_{10}S_2$
16	—	Met	—	0.22	4.7 ± 0.3	$C_{28}H_{38}N_6O_6S_2{\cdot}2\ C_2HF_3O_2$
17	Boc	D-Met	—	3.86	ND	$C_{38}H_{54}N_6O_{10}S_2$
18	—	D-Met	—	0.22	5.0 ± 0.1	$C_{28}H_{38}N_6O_6S_2{\cdot}2C_2HF_3O_2$
19	Boc	Lys	Boc	>6.00	ND	$C_{50}H_{76}N_8O_{14}$
20	—	Lys	—	−0.68	27.7 ± 1.0[d,e]	$C_{30}H_{44}N_8O_6{\cdot}4C_2HF_3O_2$
AT	—	—	—	0.59	21.4 ± 0.1	—
MX	—	—	—	0.24	25.3 ± 1.0[f]	—

[a] The predicted Clog *P* values were calculated using Clog *P* module in ChemDraw Ultra® version 6.0.1, CambridgeSoft.Com.
[b] BAC concentrations in the test solutions were 20 μM unless otherwise specified.
[c] ND, not determined.
[d] The concentration of compound **20** in the test solutions was 5 μM.
[e] Biphasic melting curves were recorded.
[f] The concentration of MX in the test solutions was 10 μM.

Table 2. Growth inhibition of BACs against human cancer cell lines

No.	GI_{50}[a] (μM)						
	MCF-7[b]		NCI-H460[b]		SF-268[b]		PC-3[c]
1	ND		ND		ND		>30
2	60%		66%		53%		1.50
3	95%		101%		107%		>30
4	71%		52%		58%		>30
5	59%		15%	2.71	70%		>10
6	35%	8.18	48%	6.08	42%	6.46	3.67
7	95%		96%		96%		>10
8	93%		54%		82%		2.23
9	66%		56%		53%		3.97
10	49%	3.85	58%		45%	2.13	1.83
11	83%		79%		79%		>10
12	68%		88%		74%		>10
13	103%		98%		97%		>30
14	68%		100%		82%		>30
15	92%		96%		98%		ND
16	0%	1.64	1%	0.38	1%	0.35	0.28
17	92%		104%		106%		ND
18	92%		94%		100%		>10
19	79%		99%		65%		>10
20	55%		31%	1.38	42%	2.03	0.83
AT	34%	4.97	22%	2.55	6%	2.45	8.52
MX	19%	3.93	8%	1.29	2%	0.97	0.78

[a] ND, not determined.
[b] Initial screening of cytotoxicity for BACs in a concentration of 4 μg/mL was conducted to determine the percentage of growth for MCF-7, NCI-H460, and SF-268 cancer cell lines. For those BACs that demonstrated growth inhibition more than 50% at the screening concentration (4 μg/mL), the GI_{50} values were determined.
[c] For those BACs demonstrated growth inhibition less than 50% against PC-3 cell line at the range of concentrations tested, the highest concentrations of the ligands used in the assay are shown.

groups seemed to be the most critical factors for the cytotoxicity of AACs for PC-3 cell line. With the exception of AAC **10**, the active AACs (**2**, **6**, **8**, and **9**) possessed free α-amino groups and lipophilic terminals (side chains), while the AACs with either protected α-amino groups (i.e., **1** and **5**) or negative C log *P* values (i.e., **7** and **11**) were inactive.

The unprotected L-Met–MAC **16** and L-Lys–MAC **20** were much more potent than their corresponding AACs **2** and **11**. The L-Met-substituted MAC **16** was the most potent compound among the BACs in this study and demonstrated much better growth-inhibition activity than AT and MX (3–30- and 2–3-fold, respectively) in all tumor cell lines.

In contrast to Lys–AACs **10** and **11**, N^{α}, N^{ε}-protected L-Lys-MAC **19** did not demonstrate significant cytotoxicity against cancer cell lines, whereas unprotected L-Lys–MAC **20** showed much stronger growth inhibition activity than AT and as potent as MX against NCI-H460, SF-268, and PC-3 cell lines. Previously, it has been reported that Lys–MAC **20** showed potent DNA binding and was effective in HL60 tumor cell killing.[12,13]

The cytotoxicity of D-amino acid-containing BACs was also studied, as the D-enantiomers not only possessed comparable DNA binding properties to the L-enantiomers, but may also be less susceptible to enzymatic hydrolysis. However, all D-amino acid-conjugated AACs and MACs were inactive in the growth inhibition against various human cancer cell lines. In contrast to the DNA thermal denaturation study, in which the chirality did not demonstrate any significant influence on the T_m, the chirality played a critical role in the cytotoxicity of BACs. A clear discrimination in the results between the L- and D-enantiomers was observed, in which the L-isomers were always much more effective than the corresponding D-isomers.

4. Discussion

In this study, three strategies were used to design BACs with higher antitumor activity. The sulfur-containing Met–MAC **16** had higher cytotoxicity than MX, while **16** was a much weaker DNA binder than MX. These results suggested that the conjugation of methionine to the anthraquinone moiety altered the pharmacological profiles of AT and MX. Classical antitumor anthraquinone derivatives, such as AT and MX, can bind to DNA tightly by intercalation, whereas it is not clear whether or how this binding results in their antiproliferative effects. In addition, the notion that the ability to increase the melting temperature of DNA did not correlate with the antitumor activity was also reported.[10,13] Therefore, the potent antiproliferative effects of Met–MAC **16** against tumor cells may be more a function of their ability to interfere with other cellular targets (e.g., TOP2) than their ability to intercalate with DNA. The quite different pharmacological profile of the Met–MAC **16**, in which different mechanisms of cytotoxicity might be involved, pointed to a novel type of antineoplastic pharmacophore which gives promise to eliminate the severe problem of cardiotoxicity for MX.

The DNA binding of hydroxyl-containing AACs **7** and **9** was substantially stronger than that of Met–BACs but weaker than that of AT. Under physiological conditions, the positively charged Lys–BACs were the strongest DNA binders in the series. However, this ability was not completely reflected in the antitumor activity of Lys–BACs. In general, more polar amino acid-containing BACs displayed higher T_m. Therefore, the ΔT_m values of the BACs were in the order of Lys $\gg$ Ser $\geqslant$ Tyr > Met. In contrast to DNA binding, the more lipophilic BACs were more potent in killing cancer cells in both the AAC and MAC series. Moreover, all the D-BACs were inactive in inhibition of cancer cell growth irrespective of their ability to stabilize ct-DNA. Considering that all inactive N^{α}-unprotected BACs were either in D-configuration or with negative C log *P* values, these inactive BACs might have poorer accessibility (e.g., penetration, uptake, etc.) to tumor cells.

Both AT and MX have been well established as TOP2-targeting anticancer drugs and induce TOP2-mediated DNA breakage. We therefore evaluated the abilities of MAC **16** in generation of DNA damage and cytotoxicity by the comet assay[30] and MTT assay.[31] The potential contribution of TOP2 in mediating the effect of MAC **16** was further investigated with the mutant HL-60/MX-2 cell line that was known to have reduced levels of both TOP2 isozymes and consequently leading to cross-resistance to all known TOP2 poisons, but not other anticancer drugs.[30,32] In Figure 1, the extents of DNA breakage of chromosome DNA in HL-60/MX-2 cells treated with etoposide (VP-16), AT, MX, and MAC **16** were greatly reduced compared to that in parental HL-60 cells. In marked contrast, the TOP1-targeting drug, camptothecin (CPT), induced similar extent of DNA damage in both cell lines. Similar conclusion was obtained using PFGE analysis to examine the ability of MAC in TOP2-mediated excision of the loop-sized DNA fragments[31] (data not shown). These results

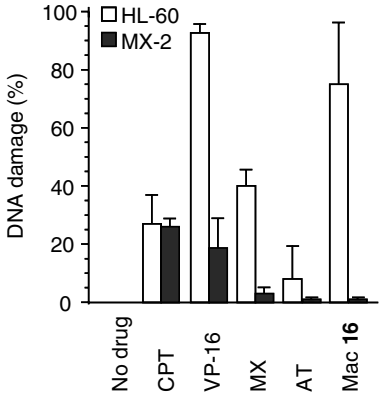

Figure 1. Drug-induced strand breaks in chromosomal DNA in HL-60 and TOP2-deficient HL-60/MX-2 cell lines.[33] DNA damage (%): the percentage of cells showing the comet image, which corresponded to damaged chromosomal DNA.

Table 3. Growth inhibition against HL-60 and TOP2-deficient HL-60/MX-2 cell lines[a,b]

Compound[c]	GI_{50} (nM)		GI_{50} ratio
	HL-60	HL-60/MX-2	
CPT	1.7	1.5	0.9
VP-16	140	5980	43
AT	29	430	15
MX	0.33	26	79
MAC **16**	0.32	12	38

[a] Determined by the MTT cytotoxic assay.[31]
[b] HL-60: leukemia cell line.
[c] CPT, camptothecin; VP-16, etoposide.

strongly suggest that TOP2s are primarily responsible for DNA breakage induced by MAC **16** treatment. Consistently, HL-60/MX-2 cells were also shown to be cross-resistant to VP-16, AT, MX, and MAC **16** (GI_{50} ratio = 15- to 79-fold), but not to CPT (GI_{50} ratio = 0.9-fold) as shown in Table 3. Taken together, we conclude that the cytotoxic action of these BACs was most likely through poisoning of the TOP2s.

5. Conclusion

L-Met–MAC **16** was the most potent inhibitor of tumor cell growth in the BACs, whereas **16** only showed limited DNA binding. The cytotoxicity of MAC **16** was higher than that of MX, while the T_m of MAC **16** was much lower than that of MX. These results suggested a quite different pharmacological profile, which may provide opportunities to develop novel anthraquinone derivatives with increased potency and lower toxicity. In contrast to MAC **16**, L-Lys–MAC **20** demonstrated higher T_m than MX and a similar cytotoxicity as MX. These data supported that the ability to stabilize DNA is not parallel to the ability to kill cancer cells. Non-selective DNA intercalation of classical anthraquinone antitumor agents has resulted in various adverse reactions in clinic. Based on the SAR established in this study, the DNA binding and the cytotoxicity could be separated and thus, MAC **16** may provide a lead for the development of new generations of anthraquinone-type antitumor agents. Additional data from further pharmacological studies suggest that the cytotoxicity of MAC **16** was most likely through poisoning of the TOP2s.

6. Experimental

6.1. General procedures

Melting points were determined on a MEL-TEMP II apparatus by Laboratory Devices and are uncorrected. NMR spectra were recorded on Bruker DPX-200 and AMX-400 FT–NMR spectrometers. Chemical shifts are expressed in parts per million (ppm) on the δ scale relative to a tetramethylsilane (TMS) internal standard. Fast atom bombardment mass (FABMS) spectra were recorded on a JEOL SX-102A GC/LC/Mass spectrometer. High-resolution FABMS measurements were obtained using a Finnigan/Thermo Quest MAT 95XL mass spectrometer. Elemental analyses were performed with a Heraeus varioIII-NCSH instrument and were within ±0.4% for the elements indicated. Thin-layer chromatography (TLC) was performed on Merck (art. 5715) silica gel plates and visualized under UV light (254 nm), upon treatment with iodine vapor, or upon heating after treatment with 5% phosphomolybdic acid in ethanol. Flash column chromatography was performed with Merck (art. 9385) 40–63 μm silica gel 60. Anhydrous tetrahydrofuran was distilled from sodium-benzophenone prior to use. No attempt was made to optimize yields.

6.2. General synthetic methods

6.2.1. Synthetic method A. (*S*,*S*)-1,4-Bis[2-[2,6-bis(*tert*-butoxycarbonylamino)hexanoylamino]ethylamino]-9,10-anthracenedione (10). *N*-α,ε-Di-*t*-Boc-L-lysine dicyclohexylammonium salt (1.35 g, 2.55 mmol), dicyclohexylcarbodiimide (DCC, 551 mg, 2.67 mmol), and HOBt (375 mg, 2.78 mmol) were dissolved in CH_2Cl_2 (10 mL) and stirred for 1 h at room temperature. The white precipitate (*N*,*N*′-dicyclohexylurea) was removed by filtration, and then the filtrate was added to a stirred solution of **25** (376 mg, 1.16 mmol) and triethylamine (1.30 mL) in CH_2Cl_2 (5 mL). After being stirred for 17 h at room temperature, the solvent was removed under reduced pressure. The residue was purified by flash column chromatography (silica gel, MeOH/CH_2Cl_2 = 1:10) to afford **10** (723 mg, 64%) as a deep blue solid. Mp 196–198 °C; ^{1}H NMR (200 MHz, DMSO-d_6) δ 1.05–1.42 (m, 44H), 1.45–1.70 (m, 4H), 2.70–2.92 (m, 4H), 3.12–3.41 (m, 4H), 3.45–3.65 (m, 4H), 3.73–3.96 (m, 2H), 6.64–6.86 (m, 4H), 7.55–7.65 (m, 2H), 7.72–7.84 (m, 2H), 8.08 (br s, 2H), 8.17–8.28 (m, 2H), 10.81 (br s, 2H); ^{13}C NMR (100 MHz, DMSO-d_6) δ 22.8, 28.1, 28.2, 29.2, 31.7, 38.9, 39.5, 41.2, 54.4, 77.2, 77.9, 108.7, 124.4, 125.7, 132.3, 133.8, 145.9, 155.3, 155.5, 172.7, 180.8; FABHRMS Calcd for $C_{50}H_{76}N_8O_{12}$ $[M]^+$ 980.5583. Found: 980.5547.

6.2.2. Synthetic method B. (*S*,*S*)-1,4-Bis[2-(2,6-diaminohexanoyl-carbamoyl)ethylamino]-9,10-anthracenedione trifluoroacetate (11). Compound **10** (255 mg, 0.260 mmol) was treated with a mixture of CH_2Cl_2 (5 mL) and trifluoroacetic acid (5 mL) and stirred at room temperature for 30 min. The resulted solution was evaporated to dryness under high vacuum to give **11** (225 mg, 84%) as a blue oil. ^{1}H NMR (200 MHz, DMSO-d_6) δ 1.25–1.42 (m, 4H), 1.42–1.61 (m, 4H), 1.61–1.82 (m, 4H), 2.65–2.86 (m, 4H), 3.44–3.68 (m, 8H), 3.68–3.85 (m, 2H), 7.59 (s, 2H), 7.80–7.84 (m, 8H), 8.22–8.24 (m, 8H), 8.82 (br s, 2H), 10.81 (br s, 2H); ^{13}C NMR (100 MHz, DMSO-d_6) δ 21.3, 26.6, 30.5, 38.4, 38.8, 41.2, 52.2, 109.0, 124.4, 125.8, 132.6, 133.8, 145.8, 169.0, 181.1; FABHRMS Calcd for $C_{30}H_{45}N_8O_4$ $[M+H]^+$ 581.3564. Found: 581.3574.

6.2.3. Synthetic method C. (*S*,*S*)-l,4-Bis[2-(2-amino-3-*tert*-butoxy-propionylamino)ethylamino]-9,10-anthracenedione (6). Compound **5** (120 mg, 0.114 mmol) was treated with a solution of 10% piperidine in CH_2Cl_2 (5 mL) for 40 min at room temperature, and then the solvent was

removed under reduced pressure. The crude residue was chromatographed (silica gel, MeOH/CH_2Cl_2 = 1:5) to afford **6** (50.4 mg, 73%) as a blue solid. Mp 159 °C; ^{1}H NMR (200 MHz, $CDCl_3$) δ 1.17 (s, 18H), 1.66–1.85 (m, 4H), 3.42–3.62 (m, 10H), 3.62–3.76 (m, 4H), 7.30 (s, 2H), 7.62–7.67 (m, 2H), 8.01 (s, 2H), 8.19–8.24 (m, 2H), 10.72 (s, 2H); ^{13}C NMR (100 MHz, $CDCl_3$) δ 27.5, 39.0, 42.0, 55.6, 63.9, 73.4, 110.4, 123.6, 126.1, 132.2, 134.4, 146.1, 173.9, 182.8; FABHRMS Calcd for $C_{32}H_{47}N_6O_6$ $[M+H]^+$ 611.3557. Found: 611.3555.

6.3. (*S*,*S*)-l,4-Bis[2-(2-*tert*-butoxycarbonylamino-4-methylsulfanyl-butyrylamino)ethylamino]-9,10-anthracenedione (1)

Compound **1** was synthesized using *N*-α-*t*-Boc-L-methionine and **25** according to the synthetic method A as a blue solid in a yield of 64%. Mp 236–237 °C; ^{1}H NMR (200 MHz, DMSO-d_6) δ 1.36 (s, 18H), 1.61–1.87 (m, 4H), 1.96 (s, 6H), 2.30–2.45 (m, 4H), 3.25–3.30 (m, 4H), 3.40–3.60 (m, 4H), 3.81–4.00 (m, 2H), 6.96 (d, J = 8.0 Hz, 2H), 7.59 (s, 2H), 7.77–7.79 (m, 2H), 8.01–8.12 (m, 2H), 8.22–8.26 (m, 2H), 10.79–10.82 (m, 2H); FABHRMS Calcd for $C_{38}H_{54}N_6O_8S_2$ $[M]^+$ 786.3445. Found: 786.3439. Anal. Calcd for $C_{38}H_{54}N_6O_8S_2$: C, 57.99; H, 6.92; N, 10.68. Found: C, 57.94; H, 6.96; N, 10.44.

6.4. (*S*,*S*)-l,4-Bis[2-(2-amino-4-methylsulfanyl-butyrylamino)ethylamino]-9,10-anthracenedione trifluoroacetate (2)

Compound **2** was synthesized using compound **1** according to the synthetic method B as a blue solid in a yield of 98%. Mp 178–180 °C; ^{1}H NMR (200 MHz, DMSO-d_6) δ 1.95 (s, 6H), 1.99–2.03 (m, 4H), 2.41–2.45 (m, 4H), 3.32–3.36 (m, 4H), 3.54–3.72 (m, 4H), 3.74–3.88 (m, 2H), 7.57 (s, 2H), 7.79–7.83 (m, 2H), 8.20–8.23 (m, 2H), 8.25–8.27 (m, 6H), 8.73–8.82 (m, 2H), 10.82 (br s, 2H); ESIMS *m*/*z* 587 (MH^+). Anal. Calcd for $C_{28}H_{38}N_6O_4S_2 2CF_3CO_2H 1.5H_2O$: C, 45.66; H, 5.15; N, 9.98. Found: C, 45.55; H, 5.09; N, 9.84.

6.5. (*R*,*R*)-l,4-Bis[2-(2-*tert*-butoxycarbonylamino-4-methylsulfanyl-butyrylamino)ethylamino]-9,10-anthracenedione (3)

Compound **3** was synthesized using *N*-α-*t*-Boc-D-methionine and **25** according to the synthetic method A as a blue solid in a yield of 63%. Mp 233–236 °C; FABHRMS Calcd for $C_{38}H_{54}N_6O_8S_2$ $[M]^+$ 786.3445. Found: 786.3429.

6.6. (*R*,*R*)-l,4-Bis[2-(2-amino-4-methylsulfanyl-butyrylamino)ethylamino]-9,10-anthracenedione trifluoroacetate (4)

Compound **4** was synthesized using compound **3** according to the synthetic method B as a blue solid in a yield of 100%. Mp 68–71 °C (free base); FABHRMS Calcd for $C_{28}H_{39}N_6O_4S_2$ $[M+H]^+$ 587.2474. Found: 587.2484.

6.7. (*S*,*S*)-l,4-Bis[2-[3-*tert*-butoxy-2-(9*H*-fluoren-9-ylmethoxycarbonylamino)-propionylamino]ethylamino]-9,10-anthracenedione (5)

Compound **5** was synthesized using *N*-α-Fmoc-*O*-*t*-butyl-L-Serine and **25** according to the synthetic method A as a blue solid in a yield of 54%. Mp 156–158 °C; ^{1}H NMR (200 MHz, DMSO-d_6) δ 1.05 (s, 18H), 3.31–3.32 (m, 4H), 3.38–3.42 (m, 4H), 3.48–3.52 (m, 4H), 4.05–4.10 (m, 4H), 4.20–4.24 (m, 2H), 4.24–4.30 (m, 2H), 7.28–7.56 (m, 16H), 7.68–7.72 (m, 6H), 7.84–7.88 (m, 2H), 8.17–8.19 (m, 2H), 10.75–10.79 (m, 2H); FABHRMS Calcd for $C_{62}H_{66}N_6O_{10}$ $[M]^+$ 1054.4840. Found: 1054.4838.

6.8. (*S*,*S*)-l,4-Bis[2-(2-amino-3-hydroxy-propionylamino)ethylamino]-9,10-anthracenedione trifluoroacetate (7)

Compound **7** was synthesized using compound **6** according to the synthetic method B as a blue oil in a yield of 100%. ^{1}H NMR (200 MHz, DMSO-d_6) δ 1.58–1.63 (m, 4H), 2.83–3.05 (m, 6H), 3.49–3.62 (m, 4H), 3.75–3.79 (m, 2H), 7.57 (s, 2H), 7.81 (dd, J = 5.9, 3.3 Hz, 2H), 8.12 (br s, 6H), 8.24 (dd, J = 5.9, 3.3 Hz, 2H), 8.71 (t, J = 6.0 Hz, 2H), 10.80 (t, J= 6.0 Hz, 2H); FABHRMS Calcd for $C_{24}H_{31}N_6O_6$ $[M+H]^+$ 499.2305. Found: 499.2302.

6.9. (*S*,*S*)-l,4-Bis[2-[2-amino-3-(4-*tert*-butoxyphenyl)-propionylamino]ethylamino]-9,10-anthracenedione (8)

Compound **8** was synthesized using *N*-α-Fmoc-*O*-*t*-butyl-L-tyrosine and **25** according to the synthetic method A followed by the general procedure C, as a blue solid in a yield of 48%. Mp 150–152 °C; ^{1}H NMR (200 MHz, $CDCl_3$) δ 1.32 (s, 18H), 2.67 (dd, J = 13.8, 9.5 Hz, 2H), 3.24 (dd, J = 13.7, 3.9 Hz, 2H), 3.49 (s, 4H), 3.55–3.65 (m, 10H), 6.92 (d, J = 8.4 Hz, 4H), 7.11 (d, J = 8.4 Hz, 4H), 7.35 (s, 2H), 7.65–7.70 (m, 4H), 8.26–8.31 (m, 2H), 10.78 (br s, 2H); FABHRMS Calcd for $C_{44}H_{55}N_6O_6$ $[M+H]^+$ 763.4183. Found: 763.4172.

6.10. (*S*,*S*)-l,4-Bis[2-[2-amino-3-(4-hydroxyphenyl)-propionylamino]ethylamino]-9,10-anthracenedione trifluoroacetate (9)

Compound **9** was synthesized using compound **8** according to the synthetic method B as a blue solid in a yield of 99%. Mp 169–171 °C; ^{1}H NMR (200 MHz, DMSO-d_6) δ 2.80–3.03 (m, 4H), 3.25–3.55 (m, 8H), 3.85–3.96 (m, 4H), 6.68 (d, J = 8.4 Hz, 4H), 7.02 (d, J = 8.4 Hz, 4H), 7.55 (s, 2H), 7.77–7.83 (m, 2H), 8.13–8.28 (m, 8H), 8.70–8.77 (m, 2H), 10.77 (br s, 2H); FABHRMS Calcd for $C_{36}H_{39}N_6O_6$ $[M+H]^+$ 651.2931. Found: 651.2917.

6.11. (*R*,*R*)-l,4-Bis[2-[6-*tert*-butoxycarbonylamino-2-(9*H*-fluoren-9-ylmethoxycarbonylamino)-hexanoylamino]ethylamino]-9,10-anthracenedione (12)

Compound **12** was synthesized using *N*-α-Fmoc-*N*-ε-*t*-Boc-D-lysine and **25** according to the synthetic method A as a blue solid in a yield of 41%. Mp 155–156 °C; ^{1}H NMR (200 MHz, DMSO-d_6) δ 1.33 (s, 18H), 1.50–1.70 (m, 4H), 2.79–2.90 (m, 4H), 3.08–3.19 (m, 8H), 3.28–3.30 (m, 4H), 3.51–3.53 (m, 4H), 3.81–3.98 (m, 2H), 4.04–4.20 (m, 6H), 6.72–6.75 (m, 2H), 7.18–7.56 (m, 16H), 7.63–7.78 (m, 4H), 7.84–7.88 (m, 4H), 8.10–8.22 (m, 2H), 10.65–10.80 (m, 2H); FABHRMS Calcd for $C_{70}H_{80}N_8O_{12}$ $[M]^+$ 1224.5896. Found: 1224.5895.

6.12. (*R*,*R*)-l,4-Bis[2-(2-amino-6-*tert*-butoxycarbonylamino-hexanoylamino)-ethylamino]-9,10-anthracenedione (13)

Compound **13** was synthesized using compound **12** according to the synthetic method C as a blue solid in a yield of 78%. Mp 150 °C; ^{1}H NMR (200 MHz, DMSO-d_6) δ 1.10–1.40 (m, 26H), 1.45–1.60 (m, 4H), 2.70–2.90 (m, 4H), 3.01–3.16 (m, 4H), 3.32–3.33 (m, 4H), 3.47–3.63 (m, 6H), 6.64–6.78 (m, 2H), 7.62 (s, 2H), 7.76–7.80 (m, 2H), 8.16–8.25 (m, 4H), 10.71–10.85 (m, 2H); FABHRMS Calcd for $C_{40}H_{61}N_8O_8$ $[M+H]^+$ 781.4612. Found: 781.4601.

6.13. (*R*,*R*)-l,4-Bis[2-(2,6-diamino-hexanoylamino)ethylamino]-9,10-anthracenedione trifluoroacetate (14)

Compound **14** was synthesized using compound **13** according to the synthetic method B as a blue oil in a yield of 100%. ^{1}H NMR (200 Hz, DMSO-d_6) δ 1.25–1.41 (m, 4H), 1.41–1.61 (m, 4H), 1.61–1.80 (m, 4H), 2.67–2.87 (m, 4H), 3.44–3.50 (m,4H), 3.50–3.67 (m, 4H), 3.74 (s, 2H), 7.58 (s, 2H), 7.74 (br s, 6H), 7.82 (dd, J = 5.9, 3.3 Hz, 2H), 8.15 (br s, 6H), 8.24 (dd, J = 5.8, 3.2 Hz, 2H), 8.77 (t, J = 5.0 Hz, 2H), 10.80 (t, J = 4.0 Hz, 2H); FABHRMS Calcd for $C_{30}H_{45}N_8O_4$ $[M+H]^+$ 581.3564. Found: 581.3552.

6.14. (*S*,*S*)-l,4-Bis[2-(2-*tert*-butoxycarbonylamino-4-methylsulfanyl-butyrylamino)ethylamino]-5,8-dihydroxy-9,10-anthracenedione (15)

Compound **15** was synthesized using *N*-α-*t*-Boc-L-methionine and **26** according to the synthetic method A aa a blue solid in a yield of 54%. Mp 219–220 °C; ^{1}H NMR (200 MHz, DMSO-d_6) δ 1.36 (s, 18H), 1.76–1.80 (m, 4H), 1.95 (s, 6H), 2.38–2.41 (m, 4H), 2.49–2.51 (m, 4H), 3.58–3.62 (m, 4H), 3.85–3.97 (m, 2H), 6.96 (d, J = 7.4 Hz, 2H), 7.15 (s, 2H), 7.65 (s, 2H), 8.08–8.16 (m, 2H), 10.52–10.68 (m, 2H), 13.52 (s, 2H); FABHRMS Calcd for $C_{38}H_{54}N_6O_{10}S_2$ $[M]^+$ 818.3343. Found: 818.3365.

6.15. (*S*,*S*)-l,4-Bis[2-(2-amino-4-methylsulfanyl-butyrylamino)ethylamino]-5,8-dihydroxy-9,10-anthracenedione trifluoroacetate (16)

Compound **16** was synthesized using compound **15** according to the synthetic method B as a blue solid in a yield of 98%. Mp 266–268 °C; ^{1}H NMR (400 MHz, DMSO-d_6) δ 1.90–1.97 (m, 10H), 2.42 (t, J = 7.9 Hz, 4H), 3.58–3.67 (m, 8H), 3.76–3.81(m, 2H), 7.17 (s, 2H), 7.62 (s, 2H), 8.18 (s, 6H), 8.74–8.76 (m, 2H), 10.53–10.55 (m, 2H), 13.46 (s, 2H); ^{13}C NMR (100 MHz, DMSO-d_6) δ 25.5, 28.6, 31.5, 41.4, 52.1, 62.0, 107.5, 114.8, 124.4, 125.2, 146.9, 154.6, 169.8, 183.5; FABHRMS Calcd for $C_{28}H_{39}N_6O_6S_2$ $[M+H]^+$ 619.2372. Found: 619.2380.

6.16. (*R*,*R*)-l,4-Bis[2-(2-*tert*-butoxycarbonylamino-4-methylsulfanyl-butyrylamino)ethylamino]-5,8-dihydroxy-9,10-anthracenedione (17)

Compound **17** was synthesized using *N*-α-*t*-Boc-D-methionine and **26** according to the synthetic method A as a blue solid in a yield of 69%. Mp 214–215 °C; FABHRMS Calcd for $C_{38}H_{54}N_6O_{10}S_2$ $[M]^+$ 818.3343. Found: 818.3340.

6.17. (*R*,*R*)-l,4-Bis[2-(2-amino-4-methylsulfanyl-butyrylamino)ethylamino]-5,8-dihydroxy-9,10-anthracenedione trifluoroacetate (18)

Compound **18** was synthesized using compound **17** according to the synthetic method B as a blue solid in a yield of 100%. Mp 95 °C (free base); FABHRMS Calcd for $C_{28}H_{39}N_6O_6S_2$ $[M+H]^+$ 619.2372. Found: 619.2371.

6.18. (*S*,*S*)-1,4-Bis[2-[2,6-bis(*tert*-butoxycarbonylamino)-hexanoylamino]ethylamino]-5,8-dihydroxy-9,10-anthracenedione (19)

Compound **19** was synthesized using *N*-α,ε-di-*t*-Boc-L-lysine dicyclohexylammonium salt and **26** according to the synthetic method A as a blue solid in a yield of 21%. Mp 174–176 °C; ^{1}H NMR (200 MHz, DMSO-d_6) δ 1.05–1.40 (m, 44H), 1.42–1.60 (m, 4H), 2.81 (d, J = 2.3 Hz, 4H), 3.18–3.41 (m, 4H), 3.45–3.63 (m, 4H), 3.82 (d, J = 2.3 Hz, 2H), 6.62–6.80 (m, 4H), 7.17 (s, 2H), 7.63 (s, 2H), 8.28 (br s, 2H), 10.55 (br s, 2H), 13.51 (br s, 2H); FABHRMS Calcd for $C_{50}H_{76}N_8O_{14}$ $[M]^+$ 1012.5481. Found: 1012.5523.

6.19. (*S*,*S*)-1,4-Bis[2-(2,6-diamino-hexanoylamino)ethylamino]-5, 8-dihydroxy-9,10-anthracenedione trifluoroacetate (20)

Compound **20** was synthesized using compound **19** according to the synthetic method B as a blue oil in a yield of 99%. ^{1}H NMR (200 MHz, DMSO-d_6) δ 1.16–1.40 (m, 4H), 1.40–1.61 (m, 4H), 1.61–1.82 (m, 4H), 2.58–2.82 (m, 4H), 3.24–3.54 (m, 4H), 3.54–3.82 (m, 6H), 7.18 (s, 2H), 7.64 (s, 2H), 7.85 (br s, 6H), 8.24 (br s, 6H), 8.86 (br s, 2H), 10.56 (br s, 2H), 13.50 (br s, 2H); ^{13}C NMR (100 MHz, DMSO-d_6) δ 21.2, 26.4, 30.4, 38.4, 38.7, 41.5, 52.1, 107.8, 114.8, 124.8, 125.4, 147.0, 154.7, 169.1, 183.8; FABHRMS Calcd for $C_{30}H_{45}N_8O_6$ $[M+H]^+$ 613.3462. Found: 613.3456.

6.20. Thermal denaturation of DNA[8,23,24]

Deoxyribonucleic acid sodium salt from calf thymus (ct-DNA, Type I, fibrous,) was purchased from Sigma Chemical Co., Ltd, and used without further purification. All the working solutions of ct-DNA and ligands were prepared in BPE buffer, containing 7.5 mM Na_2HPO_4, 2.5 mM NaH_2PO_4, and 1 mM EDTA, adjusted to pH 7.00 ± 0.01 using diluted hydrochloric acid. Ligands without appropriate solubility in BPE buffer were not tested. Final DNA–ligand solutions containing 100 μM of ct-DNA and 20 μM of ligands unless otherwise specified were prepared by adding concentrated ligand solutions to working solution of ct-DNA. Melting temperatures were measured by using a JASCO V-550 UV–vis spectrophotometer coupled to a JASCO temperature controller (EHC-441 and UHC-443). Samples were placed in a JASCO thermostatically controlled

cell-holder (EHC-363, 10-mm pathlength). The reduced volume quartz cuvettes (1 mL, 10-mm pathlength) were heated by circulating water. The absorbance at 260 nm was measured over the range 25–95 °C with a heating rate of 1 °C/min. Data were collected and processed using the JASCO V-550 spectra manager. The melting temperature (T_m) was taken to be the midpoint of the hyperchromic transition determined from first derivatives plots. All ΔT_m values are reported as the means ± SD from at least three determinations.

6.21. Sulforhodamine B (SRB) assays[29]

Cells were seeded in 96-well plates in medium with 5% FBS. After 24 h, cells were fixed with 10% trichloroacetic acid (TCA) to represent cell population at the time of compound addition (T_0). After additional incubation of vehicle or compound for 48 h, cells were fixed with 10% TCA and SRB at 0.4% (w/v) in 1% acetic acid was added to stain cells. Unbound SRB was washed out by 1% acetic acid and SRB bound cells were solubilized with 10 mM Trizma base. The absorbance was read at a wavelength of 515 nm. Using the following absorbance measurements, such as time zero (T_0), control growth (C), and cell growth in the presence of compound (T_X), the percentage growth was calculated at each of the compound concentration levels. Percentage growth inhibition was calculated as: $[(T_X - T_0)/(C - T_0)] \times 100$ for concentrations for which $T_X \geqslant q\ T_0$. Growth inhibition of 50% (GI_{50}) was determined at the drug concentration which resulted in 50% reduction of total protein increase in control cells during the compound incubation.

Acknowledgments

We thank Professor Shwu-Bin Lin (School of Medical Technology, College of Medicine, National Taiwan University) for the assistance in determination of T_m values and Dr. Jen-Shin Song (National Health Research Institutes) for the assistance in determination of growth inhibition of tumor cells, and acknowledge the National Science Council of the Republic of China (Grant Nos. NSC 93-2323-B-002-016 and NSC 94-2323-B-002-004) for partial financial support of this work.

References and notes

1. Willette, R. E. Analgesic Agents. In *Wilson and Gisvold's Textbook of Organic Medicinal and Pharmaceutical Chemistry*; Delgado, J. N., Remers, W. A., Eds., 10th Ed.; Lippincott-Raven: Philadelphia, 1998; pp 687–708.
2. Lown, J. W. Ed., *Anthracycline and Anthracenedione-Based Anticancer Agents*, 1988, p 402.
3. Scott, L. J.; Figgitt, D. P. *CNS Drugs* **2004**, *18*, 379.
4. Galetta, S. L.; Markowitz, C. *CNS Drugs* **2005**, *19*, 239.
5. Kluza, J.; Marchetti, P.; Gallego, M.-A.; Lancel, S.; Fournier, C.; Loyens, A.; Beauvillain, J.-C.; Bailly, C. *Oncogene* **2004**, *23*, 7018.
6. Alberts, B.; Bray, D.; Lewis, J.; Raff, M.; Roberts, K.; Watson, J. D. In *Molecular Biology of the Cell*, 3rd Ed.; Garland Publishing Inc.: New York, 1994; pp 404–416.
7. Morier-Teissier, E.; Bernier, J. L.; Lohez, M.; Catteau, J. P.; Hénichart, J. P. *Anti-Cancer Drug Des.* **1990**, *5*, 291.
8. Morier-Teissier, E.; Boitte, N.; Helbecque, N.; Bernier, J.-L.; Pommery, N.; Duvalet, J.-L.; Fournier, C.; Hecquet, B.; Catteau, J.-P.; Henichart, J.-P. *J. Med. Chem.* **1993**, *36*, 2084.
9. Meikle, I.; Cummings, J.; Macpherson, J. S.; Smyth, J. F. *Anti-Cancer Drug Des.* **1995**, *10*, 515.
10. Gatto, B.; Zagotto, G.; Sissi, C.; Cera, C.; Uriarte, E.; Palu, G.; Capranico, G.; Palumbo, M. *J. Med. Chem.* **1996**, *39*, 3114.
11. Gatto, B.; Zagotto, G.; Sissi, C.; Palumbo, M. *Int. J. Biol. Macromol.* **1997**, *21*, 319.
12. Zagotto, G.; Mitaritonna, G.; Sissi, C.; Palumbo, M. *Nucleosides Nucleotides* **1998**, *17*, 2135.
13. Zagotto, G.; Sissi, C.; Gatto, B.; Palumbo, M. *ARKIVOC* **2004**, *5*, 204.
14. Meikle, I.; Cummings, J.; Macpherson, J. S.; Hadfield, J. A.; Smyth, J. F. *Biochem. Pharmacol.* **1995**, *49*, 1747.
15. Cummings, J.; Macpherson, J. S.; Meikle, I.; Smyth, J. F. *Biochem. Pharmacol.* **1996**, *52*, 979.
16. Gresh, N.; Kahn, P. H. *J. Biomol. Struct. Dyn.* **1990**, *7*, 1141.
17. Gresh, N.; Kahn, P. H. *J. Biomol. Struct. Dyn.* **1991**, *8*, 827.
18. Silverman, R. B. DNA and DNA-Interactive Agents. In *The Organic Chemistry of Drug Design and Drug Action*, Academic Press, 1992; pp 229–232.
19. Palumbo, M.; Gatto, B.; Moro, S.; Sissi, C.; Zagotto, G. *Biochim. Biophys. Acta* **2002**, *1587*, 145.
20. Johnson, M. G.; Kiyokawa, H.; Tani, S.; Koyama, J.; Morris-Natschke, S. L.; Mauger, A.; Bowers-Daines, M. M.; Lange, B. C.; Lee, K.-H. *Bioorg. Med. Chem.* **1997**, *5*, 1469.
21. Routier, S.; Cotelle, N.; Catteau, J.-P.; Bernier, J.-L.; Waring, M. J.; Riou, J.-F.; Bailly, C. *Bioorg. Med. Chem.* **1996**, *4*, 1185.
22. Murdock, K. C.; Durr, F. E.; Citarella, R. V. *J. Med. Chem.* **1979**, *22*, 1024.
23. Zee-Cheng, R. K.-Y.; Cheng, C. C. *J. Med. Chem.* **1978**, *21*, 291.
24. Cory, M.; McKee, D. D.; Kagan, J.; Henry, D. W.; Miller, J. A. *J. Am. Chem. Soc.* **1985**, *107*, 2528.
25. Foye, W. O.; Karnik, P. S.; Sengupta, S. K. *Anti-Cancer Drug Des.* **1986**, *1*, 65.
26. Sissi, C.; Bolgan, L.; Moro, S.; Zagotto, G.; Bailly, C.; Menta, E.; Capranico, G.; Palumbo, M. *Mol. Pharmacol.* **1998**, *54*, 1036.
27. Gelus, N.; Bailly, C.; Hamy, F.; Klimkait, T.; Wilson, W. D.; Boykin, D. W. *Bioorg. Med. Chem.* **1999**, *7*, 1089.
28. Kamal, A.; Ramu, R.; Khanna, G. B. R.; Saxena, A. K.; Shanmugavel, M.; Pandita, R. M. *Bioorg. Med. Chem. Lett.* **2004**, *14*, 4907.
29. Kim, H. M.; Han, S. B.; Kim, M. S.; Kang, J. S.; Oh, G. T.; Hong, D. H. *J. Pharmacol. Toxicol. Methods* **1996**, *36*, 163.
30. Zhou, N.; Xiao, H.; Li, T.-K.; Nur-E-Kamal, A.; Liu, L. F. *J. Biol. Chem.* **2003**, *278*, 29532.
31. Li, A.; Chen, A. Y.; Yu, C.; Yong, M.; Wang, H.; Liu, L. F. *Genes Dev.* **1999**, *13*, 1553.
32. Harker, W. G.; Slade, D. L.; Parr, R. L.; Feldhoff, P. W.; Sullivan, D. M.; Holguin, H. M. *Cancer Res.* **1995**, *55*, 1707.
33. 2.5×10^5 cells of HL-60 and its TOP2-deficient variant HL-60/MX-2 were treated with CPT (10 μM), VP-16 (25 μM), AT (25 μM), MX (25 μM), or MAC **16** (25 μM) for 1 h at 37 °C. Cells were then pelleted and comet assay was performed to analyze chromosome DNA integrity. At least 50 images of nuclei were captured for each drug treatment by a CCD camera for quantitative analysis.